Supporting Information

A neutral dinuclear Ir(III) complex for anti-counterfeiting and data encryption.

Yang Jiang,[a] Guangfu Li,[a] Weilong Che,[a] Yingjie Liu,[b] Bin Xu,[b] Guogang Shan,[a] Dongxia Zhu,*[a] Zhongmin Su,*[a] Martin R. Bryce*[c]

[a.] *Key Laboratory of Nanobiosensing and Nanobioanalysis at Universities of Jilin Province, Department of Chemistry, Northeast Normal University, 5268 Renmin Street, Changchun, Jilin Province 130024, P.R. China. E-mail:* zhudx047@nenu.edu.cn; zmsu@nenu.edu.cn

[b.] *Key laboratory of supramolecular structure and materials, Institute of Theoretical Chemistry, Jilin University, Changchun 130012, P. R. China.*

[c.] *Department of Chemistry, Durham University, Durham, DH1 3LE, UK.E-mail: m.r.bryce@durham.ac.uk*

Contents:

1. Experimental - general information

Materials obtained from commercial suppliers were used without further purification unless otherwise stated. All glassware, syringes, magnetic stirring bars, and needles were thoroughly dried in a convection oven. Reactions were monitored using thin layer chromatography (TLC). Commercial TLC plates were used and the spots were visualised under UV light at 254 and 365 nm. ^{1}H NMR spectra were recorded at 25 ºC on a Varian 500 MHz spectrometer. The chemical shifts (δ) are given in parts per million relative to internal standard TMS. The ^{1}H NMR spectra were referenced internally to the residual proton resonance in DMSO-d_6 (δ 2.49 ppm) or $CDCl_3$ (δ 7.24 ppm). Powder X-ray diffraction (XRD) patterns of the samples were collected on a Rigaku Dmax 2000. Differential scanning calorimetry (DSC) curves were obtained with a NETZSCH thermal analysis DSC200 F_3 under argon with a heating rate 10 °C min^{-1}. Transmission electron microscopy (TEM) and electron diffraction analyses of the samples were obtained using a TECNAI F20 microscope. The samples were prepared by placing microdrops of the solution on a holey carbon copper grid. UV-vis absorption spectra were recorded on a Shimadzu UV-3100 spectrophotometer. Photoluminescence spectra were collected on a Shimadzu RF-5301pc spectrophotometer and Maya 2000Pro optical fiber spectrophotometer. PL efficiencies were measured with an integrating sphere (C-701, Labsphere Inc.) with a 365 nm Ocean Optics LLS-LED as the excitation source, and the laser was introduced into the sphere through an optical fiber. The excited-state lifetimes were measured by exciting the samples with 385 nm light pulses with ~3 ns pulse width from a Quanty-Ray DCR-2 pulsed Nd: YAG laser. The X-ray crystal structure data of complex **PIBIP** were collected on a Bruker Smart Apex II CCD diffractometer with graphite-monochromated Mo Kα radiation (λ = 0.71069 Å) at room temperature.

PIBIP synthesis and characterisation

Synthesis of $(ppy)_2$Ir-(bsbd)-Ir$(ppy)_2$ (PIBIP) (Scheme S1)

A yellow suspension of the dichloro-bridged diiridium complex $[Ir(ppy)_2Cl]_2$[1] (0.353 g, 0.33 mmol), bridging ligand $bsbdH_2$[2] (0.104 g, 0.33 mmol) and Na_2CO_3 (0.349 g, 3.2 mmol) in 2-ethoxyethanol was stirred at 135 ^{o}C for 6 hours under a nitrogen atmosphere and the suspension was then filtered and the precipitate was washed with diethyl ether and

water. Then the crude product was dried and purified by silica gel column chromatography with dichloromethane/methyl alcohol (10:1 v/v) as eluent. **PIBIP** was obtained as a yellow crystalline solid in 76% yield (0.315 g). ^{1}H NMR (500 MHz, DMSO-d_6, δ [ppm]): δ 8.69 (d, *J*=5 Hz, 1H); 8.56 (d, *J*=10 Hz, 1H); 8.12 (d, *J* = 10 Hz, 1H); 7.90 (d, *J* =10 Hz, 1H); 7.86 (d, *J* =10 Hz, 2H); 7.79 (s, 1H); 7.68 (d, *J* = 10 Hz, 1H); 7.32 (t, *J* = 10 Hz, 2H); 7.27 (t, *J* = 10 Hz, 1H); 7.23 (d, *J* = 5 Hz, 2H); 7.17 (t, *J* =5 Hz, 1H); 6.77 (t, *J* =10Hz, 1H); 6.59 (t, J=5Hz,1H); 6.53 (t, *J* = 10 Hz, 1H); 6.41 (d, *J* = 10 Hz, 1H); 6.37 (t, *J* =5 Hz, 1H); 6.32 (t, *J* =10 Hz, 1H); 5.98 (d, J=5 Hz,1H); 5.77 (d, *J* = 10 Hz, 1H); 5.37 (t, *J* = 5 Hz, 1H). MS: (MALDI-TOF) [m/z]: 1315.48 (calcd: 1316.29). Anal. Calcd. for $C_{64}H_{46}Ir_2N_6O_2$: C 58.43, H 3.52, N 6.39. Found C 58.56, H 3.50, N 6.41. Single crystals for X-ray analysis were grown by diffusion of acetone into a solution of **PIBIP** in dimethyl sulfoxide.

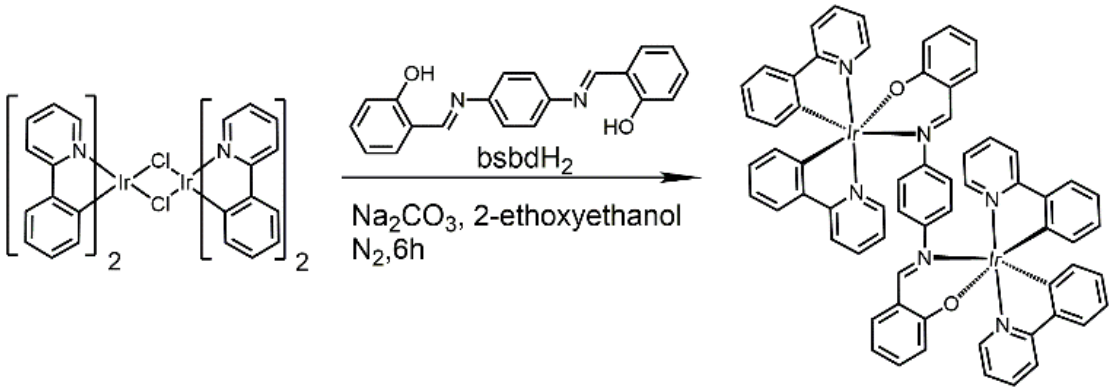

Scheme S1 Synthetic route to complex **PIBIP**.

Trademark manufacturing method

The anti-counterfeit trademark adopted the shape of a ‘flower’ comprising a central ‘stamen’ and a ‘petal’. Two specific moulds (filter paper with holes) are made for regulating the shape of as-prepared powder **MASK** and **G**. The ‘stamen’ is **MASK** and it was spread on a filter paper with a central round hole. Then remove this filter paper and substitute another one which hole is in the shape of petal. **G** is carefully spread within the hole and remove this filter paper so that the whole ‘flower’ can be demonstrated.

Procedure for conversion of **D** to **G.** **D** was ground completely by a porcelain pestle on a filter paper. It is easily hand-held because the moderate grinding strength with the pestle is easily realized by human force. The excitation illuminating sources of the anti-counterfeit trademark are always using from UV light (254 or 365nm).

2. ^{1}H NMR Spectra of PIBIP and MASK at room temperature

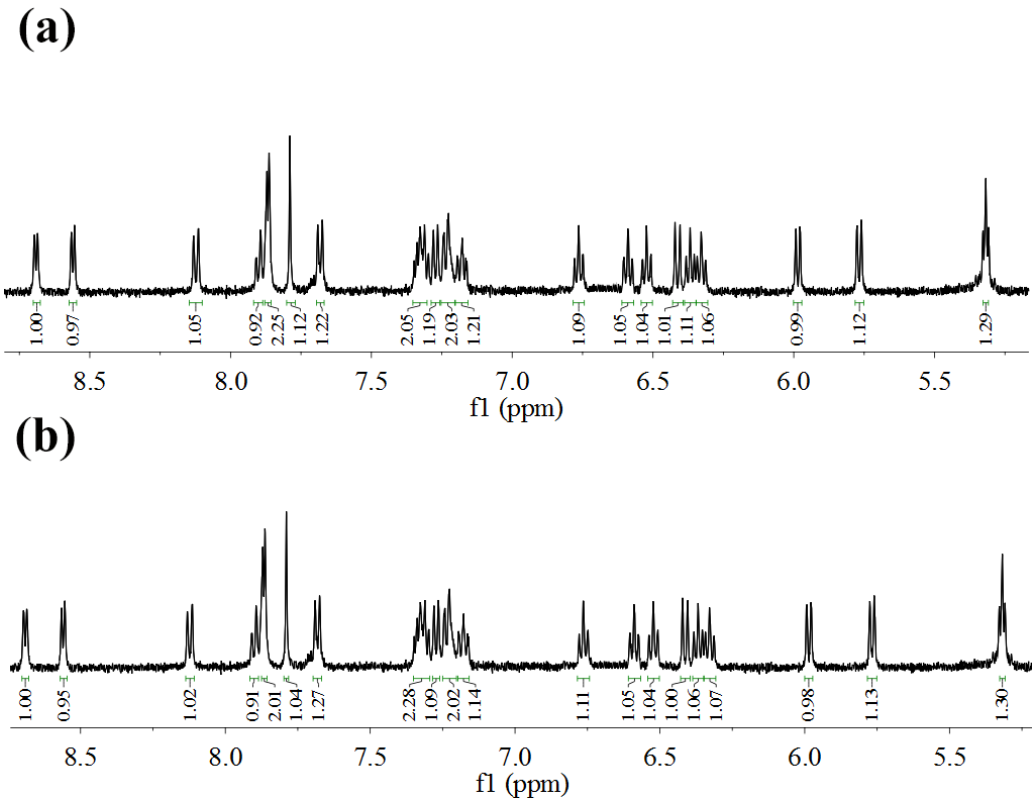

Fig. S1 ^{1}H NMR spectra of **PIBIP** in DMSO-d_6 before grinding (a) and after grinding (b).

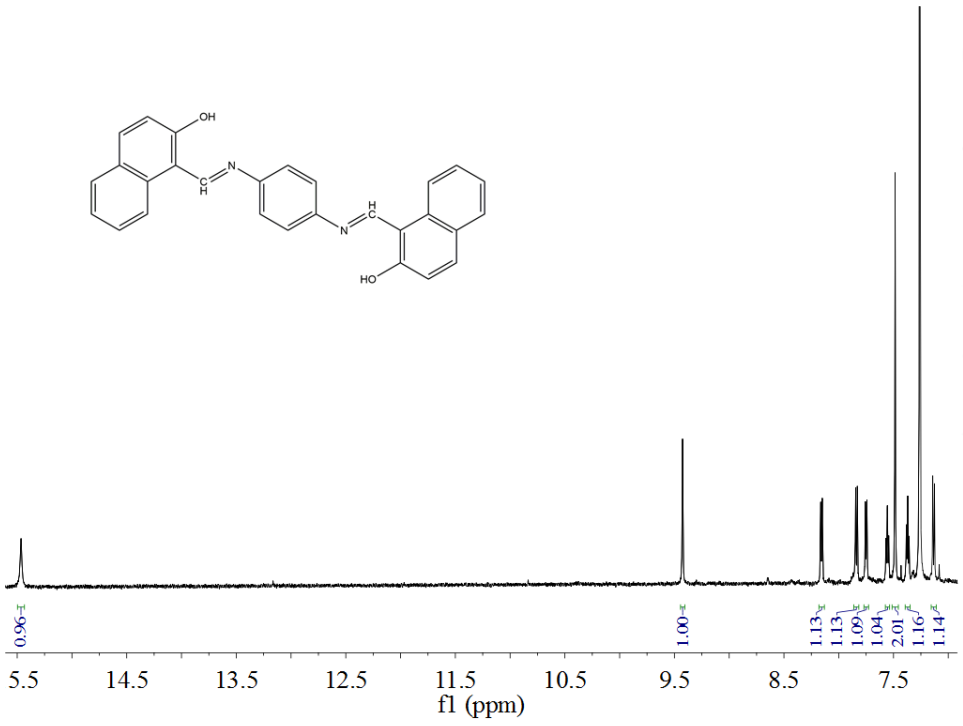

Fig. S2 ^{1}H NMR spectrum of **MASK** in $CDCl_3$ at room temperature.

3. Photophysical properties

Table S1 The phosphorescent emission efficiency (Φ_{em}) and excited-state lifetimes (τ) in various states of **PIBIP**.

	As-synthesized (**P**)	Ground (**G**)	CH_2Cl_2 wetted (**D**)	Heated (**H**)
Φ_{em}	0.20	0.07	0.26	0.19
τ (μs)	0.97	0.49	0.85	0.64

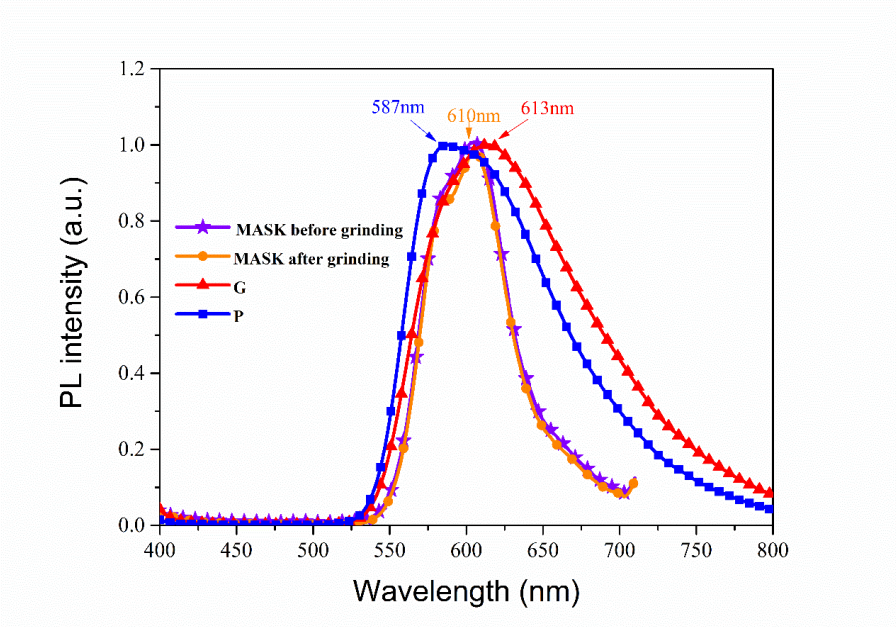

Fig. S3 The emission spectra of unground sample **MASK** and ground sample **MASK** compared with comparable states **P** and **G** of **PIBIP**.

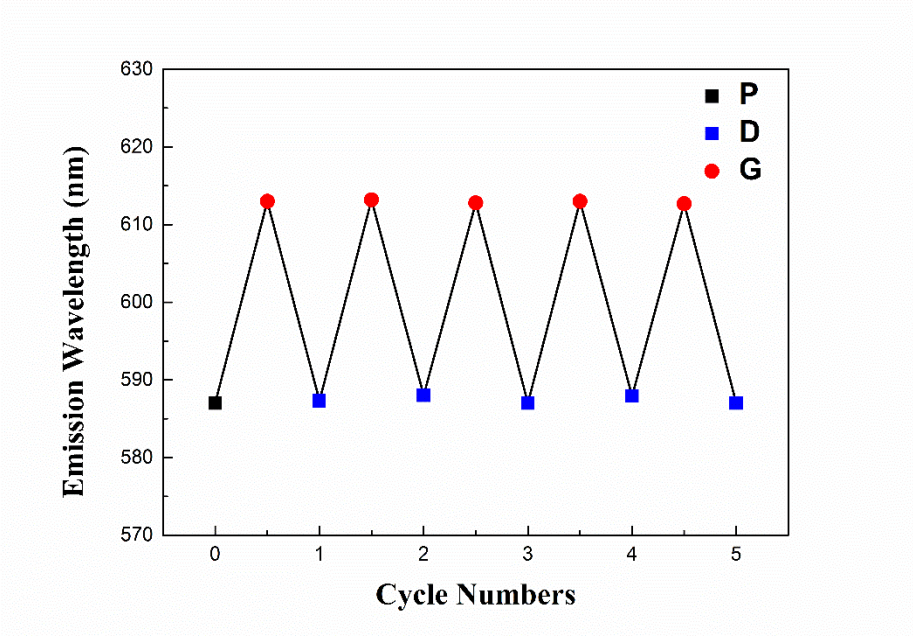

Fig. S4 Maximum emission wavelength of **PIBIP** through five cycles of states **D** and **G**.

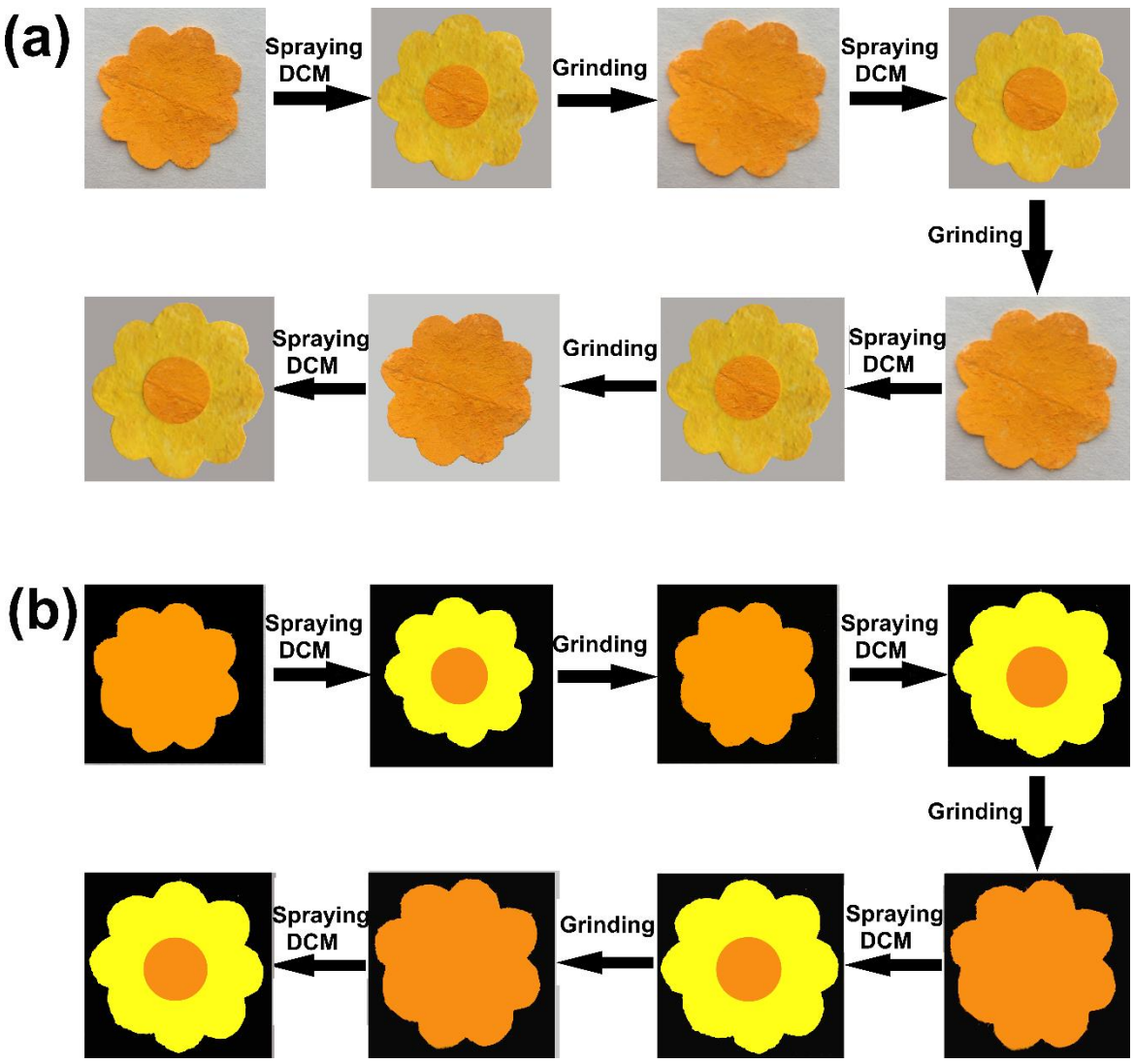

Fig. S5 Photographic images of anti-counterfeit trademark with several reversible spraying and grinding processes under (a) daylight and (b) UV light

Table S2 Photophysical characteristics of **PIBIP**.

Absorption and emission at room temperature			Emission at 77 K	$K_r \times 10^6\ s^{-1}$	$K_{nr} \times 10^6\ s^{-1}$
λ_{abs}[a](nm)	λ_{em}[b](nm)	Φ_{em}[b](τ [b][μs])	λ_{em}[c](nm)		
208(0.629), 252(0.321)	587	0.20(0.99)	584	0.20	0.80

[a]Measured in THF (1.0×10^{-5} M). [b]Measured in solid state (λ_{exc}=385 nm; error for Φ_L±5%). [c]In THF glass.

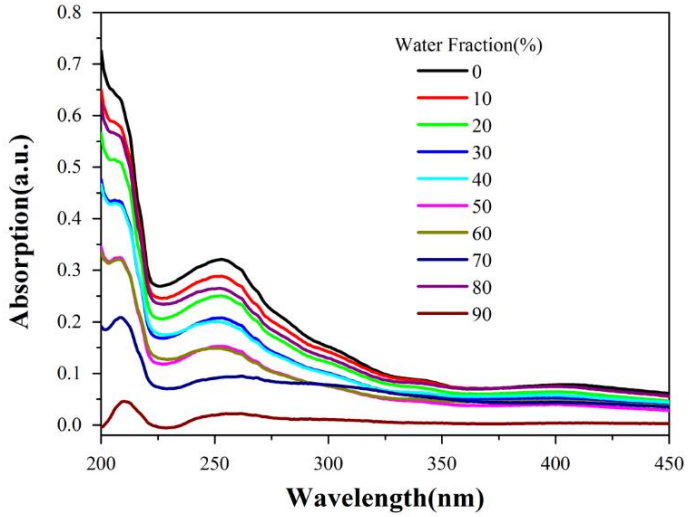

Fig. S6 UV-visible absorption spectra of **PIBIP** in acetonitrile-water mixtures with different water fractions (0-90%, v/v) at room temperature.

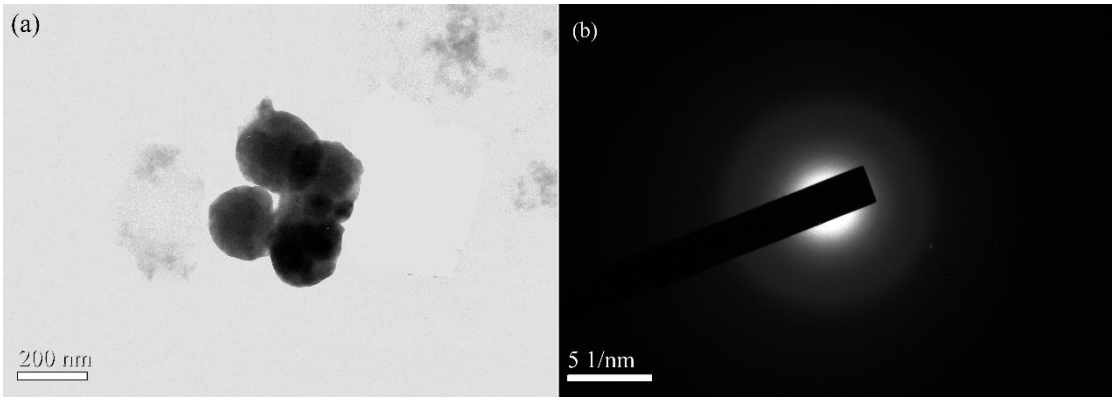

Fig. S7 (a) TEM image of nanoaggregates of **PIBIP** formed in THF–H_2O mixtures with 50% water fraction. (b) Electron diffraction pattern of the amorphous nanoaggregates.

4. X-ray crystallographic data

The molecular structure of **PIBIP** was confirmed by X-ray crystallographic analysis of single crystals. Diffraction data were collected on a Bruker SMART Apex CCD diffractometer using k(Mo-Kα) radiation (k = 0.71069 Å). Cell refinement and data reduction were made by the SAINT program. The structure was determined using the SHELXTL/PC program. The crystallographic data have been deposited with the Cambridge Crystallographic Data Centre with CCDC deposition number 1527325. These data can be obtained free of charge from The Cambridge Crystallographic Data Centre via www.ccdc.cam.ac.uk/data_request/cif.

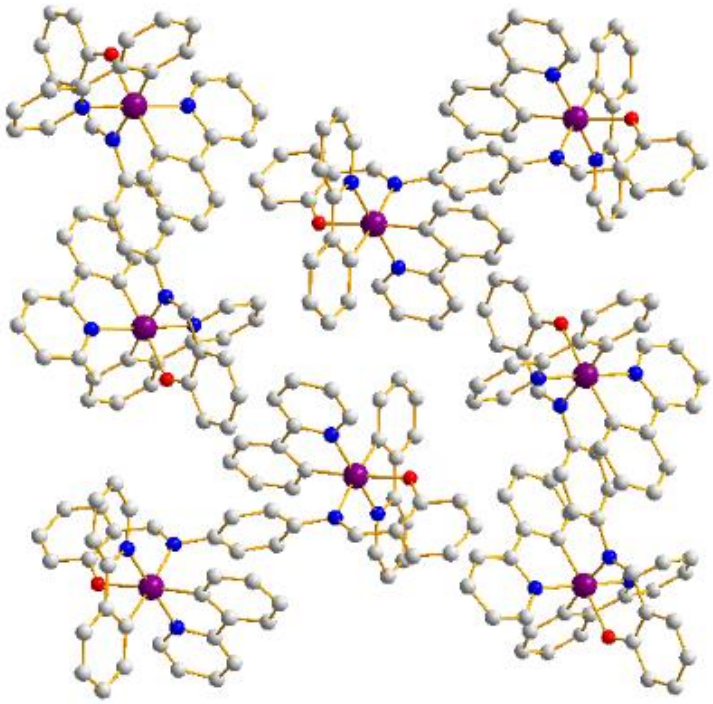

Fig. S8 Molecular packing of **PIBIP** in the crystal. Color code: Ir purple; N blue; O red**.**

Table S3 Crystal data and structure refinement for **PIBIP**.

	PIBIP
Empirical formula	$C_{64}H_{46}Ir_2N_6O_2$
Formula weight	1316.29
Temperature (K)	293(2)
Crystal system	Monoclinic
Space group	P2(1)/c
a/Å	11.434(5)
b/ Å	14.581(5)
c/ Å	18.230(5)
α/°	90.000(5)
β/°	101.210(5)
γ/°	90.000(5)
V/ $Å^3$	2981.3(18)
Z	4
$P_{calc}(g/cm^3)$	1.880
μ/mm^{-1}	6.751
R_{int}	0.0636
Goodness-of-fit on F^2	1.414
R_1[a],wR_2[b][I>2σ(I)]	0.0503, 0.1464
R_1,wR_2(all data)	0.0775, 0.1699

[a]$R_1 = \Sigma ||Fo|-|Fc|| / \Sigma |Fo|$. [b]$wR_2 = \{ \Sigma [w(Fo^2-Fc^2)^2] / \Sigma [w(Fo^2)^2] \}^{1/2}$

5. References

1. K. A. King, P. J. Spellane and R. J. Watts, *J. Amer. Chem. Soc.*, 1985, **107**, 1431-1432.

2. C. Yao, C. Niu, N. Na, D. He and J. Ouyang, *Anal. Chim. Acta*, 2015, **853**, 375-383.